



Ray picture of diffraction gratings

Alfredo Luis*, Luis Miguel Sanchez-Brea

Departamento de Óptica, Facultad de Ciencias Físicas, Universidad Complutense, 28040 Madrid, Spain

ARTICLE INFO

Article history:

Received 11 October 2008

Received in revised form 8 February 2009

Accepted 9 February 2009

PACS:

42.25.Kb

42.15.-i

42.25.Fx

42.25.Hz

Keywords:

Diffraction gratings

Geometrical optics

Wigner function

ABSTRACT

We elaborate on a geometrical picture of diffraction gratings. Exact paraxial propagation including coherence effects is obtained by allowing the geometrical rays to transport Wigner function instead of simply specific intensity. We apply this formalism to perfect and less than perfect gratings, illuminated by plane and Gaussian waves.

© 2009 Elsevier B.V. All rights reserved.

1. Introduction

Phase-space methods exemplified by the Wigner-function formalism are a powerful tool to solve problems both in quantum mechanics, quantum optics, and classical optics [1–17]. The Wigner function was originally introduced in the quantum domain but afterwards it has found a lot of applications in classical optics after being introduced to generalize the idea of radiance to partially coherent light sources [4–6]. Thus, a key feature of this approach is that it provides a useful unification of the simplicity of geometrical optics and the completeness of wave optics.

This is achieved by allowing the geometrical rays to transport Wigner function instead of just specific intensity. In particular this provides exceedingly simple propagation formulas in the paraxial domain. The Wigner function cannot represent always specific intensity, since it can take negative as well as positive values. Negative values are crucial to the completeness of the theory since they contain the coherence features [5–17]. In the Appendix we recall the basic ingredients of this formalism.

In this work we apply the Wigner-function formalism to one-dimensional gratings, both perfect and less than perfect, illuminated

by plane and Gaussian waves. More specifically, the main contributions of this analysis are:

- (i) We provide an intuitive and complete ray picture of diffraction gratings. This kind of formulation has already proven its usefulness in other interferometric problems [13,18–20].
- (ii) We show that this formalism can be extended to imperfect gratings. As deviations from perfection we consider random microscopic irregularities causing partial lack of statistical correlation between grating points [21–24].
- (iii) This analysis is also extended to partially coherent illuminating waves.
- (iv) We show that the Wigner formulation of gratings recalls the quantum angle-number Wigner function previously introduced to represent angle and angular momentum in quantum mechanics [25,26].

As recalled in (A.6) and (A.7), the effect of the grating on the input field is fully described within the geometrical picture by the Wigner function of the grating $W_T(x, p)$

$$W_T(x, p) = \frac{k}{2\pi} \int_{-\infty}^{\infty} dx' \langle T(x - x'/2) T^*(x + x'/2) \rangle \exp(ikpx'), \quad (1)$$

where $T(x)$ is the amplitude transmission coefficient, the brackets represent ensemble averages, x and x' are Cartesian coordinates orthogonal to the main propagation direction along axis z , p is the

* Corresponding author.

E-mail addresses: alluis@fis.ucm.es (A. Luis), optbrea@fis.ucm.es (L.M. Sanchez-Brea).

URLs: <http://www.ucm.es/info/gioq/alfredo.html> (A. Luis), <http://www.ucm.es/info/aocg/personal/sanchezbrea/sanchezbrea.htm> (L.M. Sanchez-Brea).

angular variable representing the local direction of propagation, and k is the wavenumber in vacuum.

A key feature of this formalism is that it includes the possibility of randomness in the diffraction process requiring statistical averages of the properties of the grating, as revealed by the averages in (1). In order to exploit this property we can decompose $T(x)$ into the product of two factors $T(x) = \tau(x)t(x)$, where $t(x)$ is a periodic, deterministic, ideal grating, while $\tau(x)$ represents either the presence of defects or the stochastic character of a real grating. In such a case we have

$$W_T(x, p) = \int_{-\infty}^{\infty} dp' W_t(x, p - p') W_\tau(x, p'). \quad (2)$$

Throughout we will consider paraxial approximation so that $W(x, p) \simeq 0$ for p outside the paraxial domain. Thus, for computational purposes the limits of the p integrals can be safely extended to $\pm\infty$ without including evanescent nonpropagating components.

When we take into account the illumination, the Wigner function for the field immediately after the plane of the diffraction object at $z = 0$ is

$$W_{TU}(x, p) = \int_{-\infty}^{\infty} dp' W_T(x, p - p') W_U(x, p'), \quad (3)$$

where $W_U(x, p)$ is the Wigner function of the illuminating light beam at $z = 0$. As illuminating field we will consider firstly a fully coherent, normally incident, scalar, and plane wave with Wigner function $W_U(x, p) \propto \delta(p)$. Then we will consider also Gaussian input wave with beam waist placed at the grating, $U(x) = \exp[-(x/\omega_0)^2]$, with Wigner function

$$W_U(x, p) = \frac{k\omega_0}{\sqrt{2\pi}} \exp\left[-2\left(\frac{x}{\omega_0}\right)^2\right] \exp\left[-\frac{1}{2}(kp\omega_0)^2\right]. \quad (4)$$

Paraxial evolution within this formalism is simply given by the constancy of W_{TU} along geometrical-optics rays. In free space for instance, the Wigner function at a plane $z > 0$ is

$$W_z(x, p) = W_{TU}(x - zp, p), \quad (5)$$

so that the irradiance at point x of the observation plane $z > 0$ can be related with the Wigner function at the grating as (see (A.3))

$$I_z(x) = \int_{-\infty}^{\infty} dp W_z(x, p) = \int_{-\infty}^{\infty} dp W_{TU}(x - zp, p). \quad (6)$$

2. Ideal grating and the angle-number Wigner function

In this section we consider in the first place a general approach to the ray picture of diffraction gratings. This is then applied to three particular examples. To begin with, let us consider ideal, perfectly periodic gratings illuminated by a normally incident, scalar plane wave, so that

$$\tau(x) = 1, \quad W_\tau(x, p) = \delta(p), \quad W_U(x, p) = \delta(p), \quad (7)$$

and

$$W_{TU}(x, p) = W_T(x, p) = W_t(x, p). \quad (8)$$

In order to compute $W_t(x, p)$ for periodic $t(x)$ with spatial period $2\pi/q$, i.e., $t(x + 2\pi/q) = t(x)$, we can use its Fourier expansion

$$t(x) = \sum_m t_m \exp(iqmx), \quad (9)$$

where m are integers, leading to

$$W_t(x, p) = \sum_{m,\ell} \delta(p - p_{\ell+m}) \exp[iqx(\ell - m)] t_m^* t_\ell, \quad (10)$$

where

$$p_{\ell+m} = (\ell + m) \frac{q}{2k}. \quad (11)$$

By introducing in Eq. (10) the unit as $1 = \sum_N \delta_{N,\ell+m}$ where N are integers we get

$$W_t(x, p) = \sum_{m,\ell} \sum_N \delta_{N,\ell+m} \delta(p - p_{\ell+m}) \exp[iqx(\ell - m)] t_m^* t_\ell. \quad (12)$$

Since $\delta_{N,\ell+m} \delta(p - p_{\ell+m}) = \delta_{N,\ell+m} \delta(p - p_N)$ we can exchange the order of sums and extract the term $\delta(p - p_N)$ out of the ℓ, m sum leading to

$$W_t(x, p) = \sum_N \delta(p - p_N) \sum_{m,\ell} \delta_{N,\ell+m} \exp[iqx(\ell - m)] t_m^* t_\ell, \quad (13)$$

which can be finally expressed as

$$W_t(x, p) = \sum_N \delta(p - p_N) \widetilde{W}_t(qx, N), \quad (14)$$

with

$$\widetilde{W}_t(\theta, N) = \sum_{m,\ell} t_m^* t_\ell \exp[i\theta(\ell - m)] \delta_{N,\ell+m}, \quad (15)$$

which can be expressed as a Wigner function as

$$\widetilde{W}_t(\theta, N) = \frac{1}{2\pi} \int_{2\pi} d\phi \exp(iN\phi) \tilde{t}(\theta - \phi) \tilde{t}^*(\theta + \phi), \quad (16)$$

$\tilde{t}(\theta)$ being the 2π -periodic function

$$\tilde{t}(\theta) = t(\theta/q) = \sum_m t_m \exp(im\theta). \quad (17)$$

Eq. (14) implies that from each point x with $\widetilde{W}_t(qx, p) \neq 0$ emerges a numerable set of rays (x, p_N) with transversal components of the ray propagation direction given by p_N in (11), where the integers N represent the ray counterpart of diffraction orders (see Fig. 1) [31,32].

In Eq. (14) we can appreciate that $\widetilde{W}_t(\theta, N)$ has essentially the same meaning than the standard definition of Wigner function (1). The only difference between them is that (16) embodies two distinctive features of ideal gratings: (i) the periodicity of the grating, represented by the replacement of the Cartesian variable x by the periodic variable θ , and (ii) the discreteness of diffraction orders, represented the replacement of the continuous variable p by the integer variable N .

It is worth noting that $\widetilde{W}_t(\theta, N)$ is quite similar to the angle-number Wigner function previously introduced in quantum mechanics to jointly represent angle and angular momentum in the plane [25,26]. However, the equivalence is not exact since the ϕ integration in (16) extends to a 2π range, while in the quantum case it extends to a π range. (Because of this we have avoided in (16) the change of variable $\phi \rightarrow \phi/2$ leading to a formula more similar to (1), since it would extend the ϕ integration to a rather unnatural 4π range.) This slight difference has some consequences. For example we have a different behavior for the θ integration of the odd and even diffraction orders

$$\int_{2\pi} d\theta \widetilde{W}_t(\theta, 2m) = |t_m|^2, \quad \int_{2\pi} d\theta \widetilde{W}_t(\theta, 2m + 1) = 0. \quad (18)$$

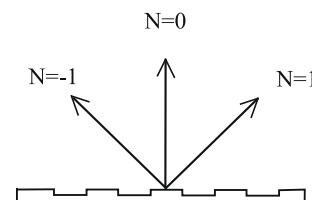


Fig. 1. The firsts three diffraction rays from a generic point of an ideal diffraction grating.

In the formal context of Wigner functions this recalls the phase-space enlargement of finite-dimensional spaces with odd dimension demanded for mathematical subtleties [27–30]. Nevertheless, in our classical-optics case (18) represents a genuine property of classical fields.

From (16) we have that negative values for the Wigner function are unavoidable for deterministic nonrandom gratings since

$$\widetilde{W}_t(\theta + \pi, N) = (-1)^N \widetilde{W}_t(\theta, N). \quad (19)$$

Negative values for the Wigner function are required for the completeness of this geometrical theory, since they embody the coherence properties of the field [12–14].

From (5), (6), and (14) we get a very simple expression for the irradiance at a point x of the plane $z > 0$, namely,

$$I_z(x) = \sum_N \widetilde{W}_t(qx_N, N), \quad (20)$$

where $x_N = x - zp_N$. This means that each observation point x is reached by a single ray from each point x_N at the grating (see Fig. 2) with weights $\widetilde{W}_t(qx_N, N)$. This provides a simple geometrical explanation of the Talbot planes z_M given by condition

$$z_M = 4\pi \frac{k}{q^2} M, \quad z_M p_N = MN \frac{2\pi}{q}, \quad (21)$$

for any integer M . Self-imaging arises in the planes z_M because the corresponding source points x_N are homologous to $x_0 = x$ (see Fig. 2), i.e., $t(x_N) = t(x)$, so that $\widetilde{W}_t(qx_N, N) = \widetilde{W}_t(qx, N)$ and

$$I_z(x) = \sum_N \widetilde{W}_t(qx_N, N) = \sum_N \widetilde{W}_t(qx, N) = I_0(x). \quad (22)$$

Then, the irradiance at z_M reproduces the radiance at $z = 0$. As shown in Refs. [32,33] the Wigner-function formalism can be also applied to analyze the fractional Talbot effects arising at distances $z_f = (4\pi k/q^2)\beta/\alpha$, where α and β are integer values [34].

2.1. Binary-amplitude grating with plane-wave coherent illumination

For the sake of illustration let us compute $\widetilde{W}_t(\theta, N)$ for an ideal amplitude grating made of transparent slits of width δx with $\delta x = 2\sigma/q$ and $2\sigma < \pi$ in an otherwise opaque plane. Restricting θ to the interval $\pi \geq \theta \geq -\pi$, we have

$$\widetilde{W}_t(\theta, N) = \frac{1}{\pi N} \sin[N(\sigma - |\theta|)], \quad \widetilde{W}_t(\theta, 0) = \frac{1}{\pi}(\sigma - |\theta|), \quad (23)$$

for $|\theta| \leq \sigma$, while for $\pi \geq |\theta| \geq \pi - \sigma$,

$$\widetilde{W}_t(\theta, N) = \frac{1}{\pi N} \sin[N(\sigma + |\theta|)], \quad \widetilde{W}_t(\theta, 0) = \frac{1}{\pi}(\sigma + |\theta| - \pi), \quad (24)$$

and $\widetilde{W}_t(\theta, N) = 0$ otherwise. In Fig. 3 we have represented $\widetilde{W}_t(\theta, N)$ for $\sigma = 1.05$ rad as a function of θ for $N = 1, 2, 3, 4$. In Fig. 4 we have represented $\widetilde{W}_t(\theta, N)$ as a function of N for $\theta = 0$ and $\theta = 0.5$, again for the same σ . In both figures we can appreciate the appearance of negative values for $\widetilde{W}_t(\theta, N)$, in agreement with (19).

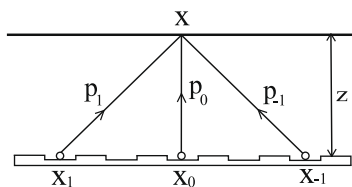


Fig. 2. Illustration of the contribution of three source points at plane $z = 0$ to the diffracted field at point x at plane $z > 0$.

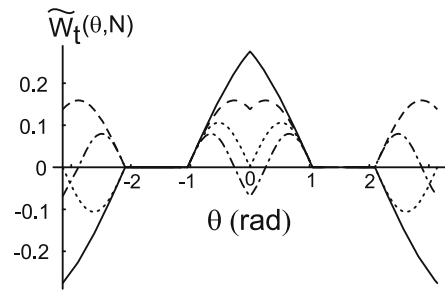


Fig. 3. $\widetilde{W}_t(\theta, N)$ in (23) and (24) as a function of θ for $N = 1$ (solid line), $N = 2$ (dashed line), $N = 3$ (dotted line), and $N = 4$ (dashed-dotted line) for $\sigma = 1.05$ rad.

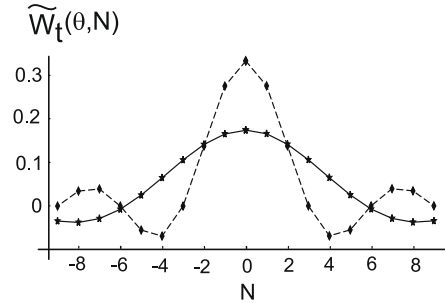


Fig. 4. $\widetilde{W}_t(\theta, N)$ in (23) and (24) as a function of N for $\theta = 0$ (dashed line) and $\theta = 0.5$ (solid line) for $\sigma = 1.05$ rad.

2.2. Sinusoidal grating with plane-wave coherent illumination

For the case of an ideal amplitude sinusoidal grating with transmission coefficient $t(x) = \cos^2(qx/2)$ the only not-null Fourier coefficients are $t_0 = 1/2$ and $t_{\pm 1} = 1/4$. In such a case, the Wigner function is

$$W_t(x, p) = \frac{1}{16} \left\{ [4 + 2 \cos(2qx)] \delta(p) + 4 \cos(qx) \left[\delta\left(p - \frac{q}{2k}\right) + \delta\left(p + \frac{q}{2k}\right) \right] + \delta\left(p - \frac{q}{k}\right) + \delta\left(p + \frac{q}{k}\right) \right\}. \quad (25)$$

This means that each point emits five rays with the following weights

$$\begin{aligned} \widetilde{W}_t(\theta, 0) &= \frac{1}{4} + \frac{1}{8} \cos(2\theta), \\ \widetilde{W}_t(\theta, \pm 1) &= \frac{1}{4} \cos \theta, \\ \widetilde{W}_t(\theta, \pm 2) &= \frac{1}{16}. \end{aligned} \quad (26)$$

According with (20) the irradiance at point x of the plane $z > 0$ is given by a suitable sum of these weights, leading to

$$I_z(x) = \frac{3}{8} + \frac{1}{2} \cos(qx) \cos\left(\frac{q^2 z}{2k}\right) + \frac{1}{8} \cos(2qx). \quad (27)$$

This equation accounts for the Talbot effect in agreement with (21) because of the z -periodicity.

2.3. Sinusoidal grating with Gaussian coherent illumination

It is also simple to determine the light distribution diffracted by sinusoidal gratings when illuminated by Gaussian beam with Wigner function $W_U(x, p)$ in (4). From (3), (4), and (25), we get that the Wigner function after the grating is

$$W_{TU}(x, p) = W_U(x, p) \frac{1}{8} [2 + g_2(p) + 4g_1(p) \cos(qx) + \cos(2qx)], \quad (28)$$

where

$$g_m(p) = \exp \left[-\frac{1}{8} (mq\omega_0)^2 \right] \cosh \left(\frac{m}{2} qkp\omega_0^2 \right). \quad (29)$$

After (6) the irradiance at $z > 0$ results

$$I_z(x) = \frac{\omega_0}{16\omega_G(z)} \{ 4h_0(x, z) + h_2(x, z) + h_{-2}(x, z) + 4h_1(x, z)f_1(z) \cos[q\Omega_1(x, z)] + 4h_{-1}(x, z)f_1(z) \times \cos[q\Omega_{-1}(x, z)] + 2h_0(x, z)f_2(z) \cos[2q\Omega_0(x, z)] \}, \quad (30)$$

where

$$\Omega_\ell(x, z) = \frac{\omega_0^2}{\omega_G(z)} \left(x - \ell \frac{qz}{2k} \right), \quad \omega_G(z) = \omega_0 \sqrt{1 + \left(\frac{z}{z_0} \right)^2}, \quad (31)$$

$$z_0 = k\omega_0^2/2, \text{ and}$$

$$f_m(z) = \exp \left[-\frac{1}{2} \left(\frac{mqz}{k\omega_G(z)} \right)^2 \right], \quad (32)$$

$$h_m(x, z) = \exp \left[-2 \left(\frac{x - \frac{mqz}{2k}}{\omega_G(z)} \right)^2 \right]. \quad (33)$$

3. Imperfect grating and effective rays

Let us consider a less than perfect grating $\tau(x) \neq 1$ illuminated by a normally incident scalar plane wave $W_U(x, p) = \delta(p)$ so that from (2), (3), and (14) we get

$$W_{TU}(x, p) = W_T(x, p) = \sum_N \widetilde{W}_T(qx, N) W_\tau(x, p - p_N). \quad (34)$$

Assuming weak imperfections in the sense that $W_\tau(x, p_N - p_M) \approx 0$ for $N \neq M$ each diffraction order N becomes a continuous distribution of rays with an angular width given by the width Δp_N of the p variable in $W_\tau(x, p)$ around p_N (see Fig. 5). In this context, weak imperfections means from (11) that $\Delta p_N < q/(2k)$.

For coherent plane-wave illumination the irradiance at $z > 0$ can be expressed as

$$I_z(x) = \sum_N \widetilde{W}_T(qx_N, N), \quad (35)$$

where the effective weights of the rays are

$$\widetilde{W}_T(qx_N, N) = \int_{-\infty}^{\infty} dp \widetilde{W}_T(qx_N - qzp, N) W_\tau(x_N - zp, p). \quad (36)$$

This implies that we can keep the idea of a diffracted field produced by the superposition of a numerable set of rays (one ray from each point x_N) provided that the weight of each ray is suitably modified. According to (36) this is given by a weighted spatial average of \widetilde{W}_T extending to the neighborhood of x_N (see Fig. 6). For the spatial stationary case [21–24] with $\langle \tau(x_1)\tau^*(x_2) \rangle$ depending only on $x_1 - x_2$ we have that (36) greatly simplifies since $W_\tau(x, p) = W_\tau(p)$ does not depend on x .

This effective-ray approach can be easily extended to the case when the light illuminating the grating is spatially stationary, so

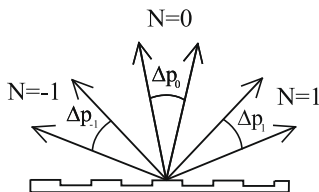


Fig. 5. Broadening of ray-diffraction orders caused by imperfect gratings.

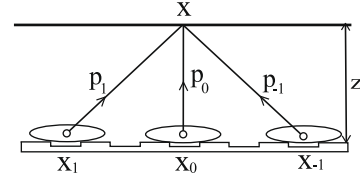


Fig. 6. Effective rays with weights depending on an area Δx_N around the source points.

its Wigner function W_U does not depend on x . Otherwise, when either W_τ or W_U depend on x , the effective-ray approach is not so useful, being then preferable to resort to the general approach.

3.1. Random sinusoidal grating with plane-wave coherent illumination

To illustrate this effective-ray approach let us consider the case of a sinusoidal grating $t(x) = \cos^2(qx/2)$ affected by random microtopography with a Gaussian characteristic function [35]

$$\langle \tau(x_1)\tau^*(x_2) \rangle = \exp \left[-\left(\frac{x_1 - x_2}{T_F} \right)^2 \right], \quad (37)$$

where $T_F = T_0/(k\sigma|n - 1|)$ being T_0 the correlation length of roughness, and σ the standard deviation of roughness. When the grating is a phase grating in transmission configuration then n is the refraction index of the grating. On the other hand, when it is a reflection grating then $n = -1$. The Wigner function of roughness is

$$W_\tau(p) = \frac{T_F k}{2\sqrt{\pi}} \exp \left[-\frac{1}{4} (T_F k p)^2 \right]. \quad (38)$$

Under plane-wave illumination the Wigner function after the grating coincides with the Wigner function of the complete grating $W_{TU} = W_T$. From (2), (25), and (38), the result for W_T is exactly of the form in (28) replacing $W_U(x, p)$ by $W_\tau(p)$ and ω_0 by $T_F/\sqrt{2}$ in $\Omega_\ell(z), f_m(z)$ and $h_m(x, z)$. Since

$$\int_{-\infty}^{\infty} dp W_\tau(p) \exp(-imqzp) = \exp \left[-\left(\frac{mqz}{T_F k} \right)^2 \right], \quad (39)$$

from (26), (36), and (38), the effective weights become

$$\begin{aligned} \widetilde{W}_T(\theta, 0) &= \frac{1}{4} + \frac{1}{8} \exp \left[-\left(\frac{2qz}{T_F k} \right)^2 \right] \cos(2\theta), \\ \widetilde{W}_T(\theta, \pm 1) &= \frac{1}{4} \exp \left[-\left(\frac{qz}{T_F k} \right)^2 \right] \cos \theta, \\ \widetilde{W}_T(\theta, \pm 2) &= \frac{1}{16}. \end{aligned} \quad (40)$$

According with (35) the irradiance at point x of the plane $z > 0$ is given by a suitable sum of these weights leading to

$$I_z(x) = \frac{3}{8} + \frac{1}{2} j_1(z) \cos(qx) \cos \left(\frac{q^2 z}{2k} \right) + \frac{1}{8} j_2(z) \cos(2qx), \quad (41)$$

where the factors $j_m(z)$ are

$$j_m(z) = \exp \left[-\left(\frac{mqz}{kT_F} \right)^2 \right]. \quad (42)$$

We can appreciate that the self-imaging effect is degraded by the randomness, that introduces exponential decaying terms.

3.2. Random sinusoidal grating with Gaussian coherent illumination

When the above stochastic grating is illuminated by the Gaussian beam in (4) the Wigner function after the grating is exactly of

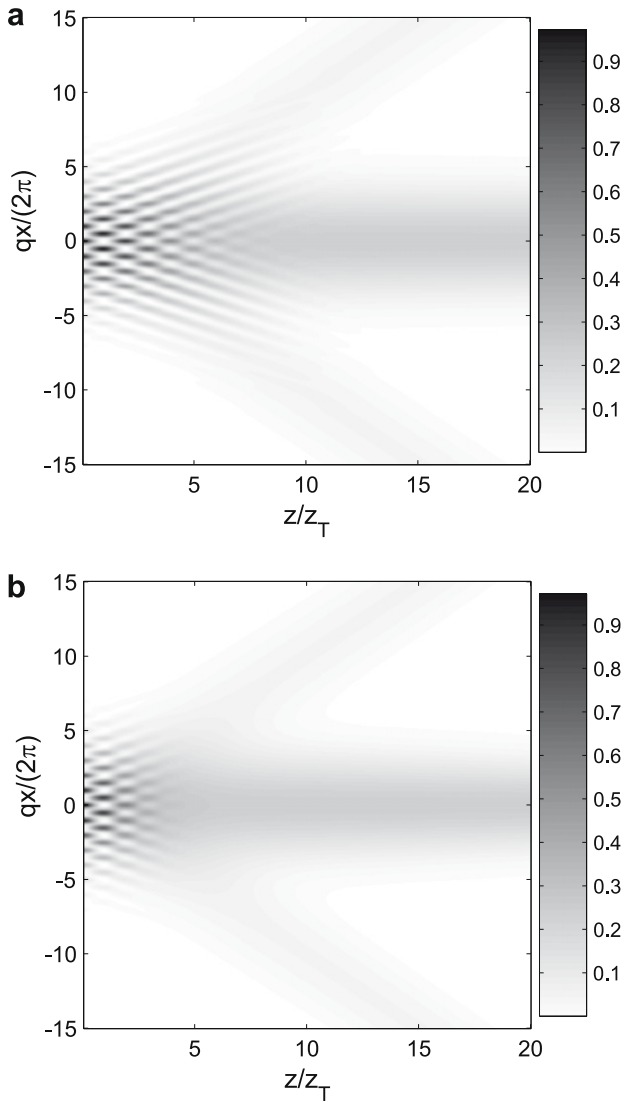


Fig. 7. Irradiance distribution in gray levels for a random diffraction grating with $q = 2\pi/10 \mu\text{m}^{-1}$ illuminated with a Gaussian wave with wavelength $\lambda = 0.632 \mu\text{m}$ and $\omega_0 = 50 \mu\text{m}$. In case (a) we have $T_F = 100 \mu\text{m}$, while in case (b) $T_F = 25 \mu\text{m}$. $z_T = z_1 = 31.6 \mu\text{m}$ is the distance from the grating to the first Talbot self-image. It can be appreciated the progressive deterioration of the self-images depending on the roughness level.

the form in (28) replacing ω_0 by $\Gamma = 1/\sqrt{2/T_F^2 + 1/\omega_0^2}$ in all the terms with p dependence. Then, the irradiance $I_z(x)$ has the same form in (30) with some changes in the parameters of the functions $\Omega_\ell(z)$, $f_m(x)$, and $h_m(x, z)$, namely

$$f_m(z) = \exp \left[-\frac{1}{2} \left(\frac{mqz\omega_0}{k\Gamma\omega_T(z)} \right)^2 \right], \quad (43)$$

$$h_m(x, z) = \exp \left[-2 \left(\frac{x - \frac{mqz}{2k}}{\omega_T(z)} \right)^2 \right], \quad (44)$$

$$\Omega_\ell(x, z) = \frac{\omega_0^2}{\omega_T^2(z)} \left(x - \ell \frac{qz}{2k} \right), \quad \omega_T(z) = \omega_0 \sqrt{1 + \left(\frac{z}{z_\alpha} \right)^2}, \quad (45)$$

and $z_\alpha = k\omega_0\Gamma/2$. When the coherence length tends to infinity $T_F \rightarrow \infty$ the randomness disappears and we have $\Gamma \rightarrow \omega_0$, $z_\alpha \rightarrow z_0$, $\omega_T \rightarrow \omega_G$, so that we recover the results of the deterministic grating in Section 2.3. On the other hand, the case of plane-wave illumination corresponds to the limit $\omega_0 \rightarrow \infty$.

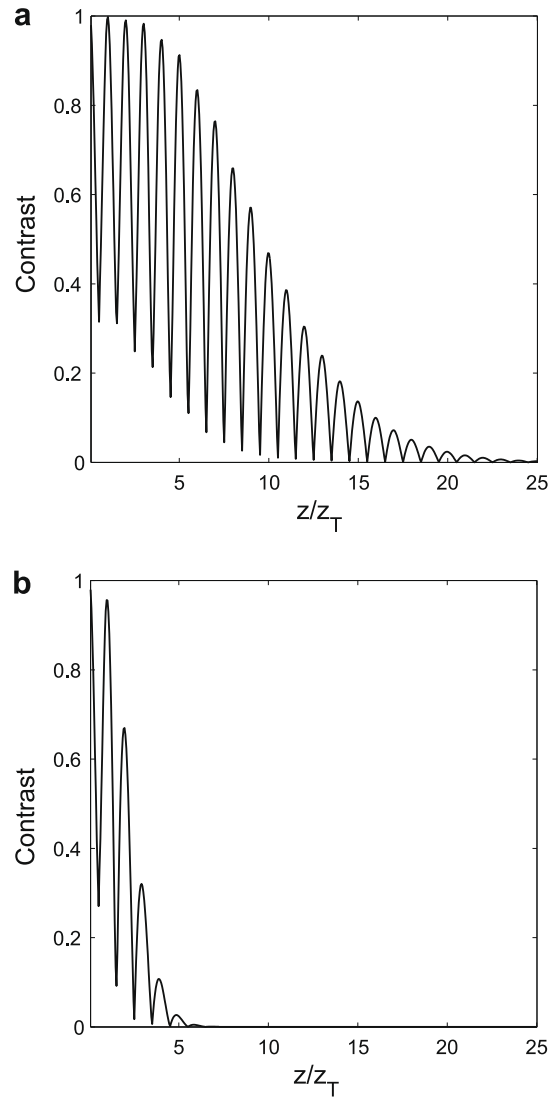


Fig. 8. Contrast of the irradiance distribution for the same cases in Fig. 7 when the grating is illuminated by a plane wave, i.e., $\omega_0 \rightarrow \infty$.

In Fig. 7 we present an example of propagation for different values of T_F . It can be appreciated that the self-images last larger propagation distances for larger T_F . This can be also appreciated in Fig. 8 that shows that the contrast of the irradiance distribution decreases exponentially for increasing distance z from the grating to the observation plane. The distance up to the contrast is not negligible decreases when T_F decreases.

4. Conclusions

In this work we have analyzed the behavior of diffraction gratings using the geometrical ray picture of light propagation provided by the Wigner-function formalism. We have applied this approach to one-dimensional gratings, both perfect and less than perfect. As deviations from perfection we have considered partial lack of statistical correlation between grating points (stochastic gratings). We have taken into account also the finite spatial width of the illuminating beam. We have shown that this formalism provides a simple and enlightening geometrical picture of diffraction-grating features such as self imaging. Therefore, this geometrical approach might be useful for simplifying calculations and analyses of diffraction by gratings under diverse conditions.

Acknowledgements

A. L. thanks support from Project No. FIS2008-01267 of the Spanish Dirección General de Investigación del Ministerio de Ciencia e Innovación.

L. M. S.-B. thanks support from Project No. CCG08-UCM/DPI-3952 of Dirección General de Universidades e Investigación de la Consejería de Educación de la Comunidad de Madrid and Universidad Complutense de Madrid.

Appendix A. Ray picture of paraxial optics

We recall the geometrical Wigner formulation of paraxial optics for scalar waves. Although standard geometrical optics excludes coherent phenomena, if we replace ray specific intensity (or radiance) by Wigner function we include once for all coherence effects. In particular we can express the degree of coherence as a functional of the Wigner function. The price to be paid is that the Wigner function can take negative values so it cannot represent always specific intensity.

A.1. Definition and properties

The Wigner function is defined as [7–11]

$$W(x, p) = \frac{k}{2\pi} \int_{-\infty}^{\infty} dx' \langle E(x - x'/2) E^*(x + x'/2) \rangle \exp(ikpx'), \quad (\text{A.1})$$

where the angle brackets represent ensemble average, x and x' are Cartesian coordinates orthogonal to the main propagation direction along axis z , p is the angular variable representing the local direction of propagation, and k is the wavenumber in vacuum. The connection between Wigner function and geometrical optics stems from the fact that x and p represent the parameters of a light ray, so that W assigns a number to each ray. The main properties of this formalism are:

- (a) The Wigner function provides complete information about second-order phenomena, including diffraction and interference, since its definition can be inverted

$$\langle E(x_1) E^*(x_2) \rangle = \int_{-\infty}^{\infty} dp W[(x_1 + x_2)/2, p] \exp[ikp(x_1 - x_2)]. \quad (\text{A.2})$$

Concerning the limits of the p integrals let us note that paraxial approximation implies $W(x, p) \simeq 0$ for p outside the paraxial domain. Thus, for computational purposes the limits of the p integrals can be safely extended to $\pm\infty$ without including evanescent nonpropagating components.

- (b) In particular, the light irradiance at a given point can be obtained by integrating the angular variables

$$I(x) = \langle |E(x)|^2 \rangle = \int_{-\infty}^{\infty} dp W(x, p). \quad (\text{A.3})$$

This is to say that the irradiance at a given point is the sum of the values of the Wigner function for all the rays passing through this point. We will refer to this sum as an *incoherent* superposition since the contributions of all rays are independent.

- (c) The Wigner function cannot represent always specific intensity, since it can take negative as well as positive values. Negative values are crucial to the completeness of the theory since they contain the coherence [7–11, 14–17].
- (d) Finally a crucial property for the geometrical interpretation of the Wigner function is that it is constant along paraxial rays

$$W_z(x', p') = W_0(x, p), \quad (\text{A.4})$$

where (x, p) and (x', p') are the input (plane $z = 0$) and output (plane z) ray parameters. In free space we have

$$W_z(x, p) = W_0(x - zp, p). \quad (\text{A.5})$$

A.2. Inverted Huygens principle

These properties can be summarized in a principle analogous to the Huygens principle but with inverted terms replacing waves by rays and coherent by incoherent superpositions. We can enunciate this principle in three steps [12, 13]:

- (i) Each point acts as a secondary source of a continuous distribution of rays with parameters x, p , $W(x, p)$. We stress that this is a continuous distribution of rays instead of the more familiar single ray at each point normal to a wavefront.
- (ii) The evolution is given by the incoherent superposition of rays, as illustrated by the example of irradiance in point (b) above. We stress that this incoherence is a key feature of the theory independent of the actual state of coherence of the light.
- (iii) The effect of spatial-local inhomogeneous filters (transparencies) altering phase and amplitude is described in the wave picture by the product of the amplitude of the input wave with a transmission coefficient $T(x)$, i.e., $U(x) \rightarrow T(x)U(x)$. In the geometrical picture this effect is described by the convolution product of the input Wigner function W_U with the Wigner function W_T of the transmission coefficient

$$W_{TU}(x, p) = \int_{-\infty}^{\infty} dp' W_T(x, p - p') W_U(x, p'), \quad (\text{A.6})$$

where

$$W_T(x, p) = \frac{k}{2\pi} \int_{-\infty}^{\infty} dx' \langle T(x - x'/2) T^*(x + x'/2) \rangle \times \exp(ikpx'), \quad (\text{A.7})$$

and we include the possibility that the transmission coefficient may require an statistical description represented by the angle brackets.

References

- [1] M. Hillery, R.F. O'Connell, M.O. Scully, E.P. Wigner, Phys. Rep. 106 (1984) 121.
- [2] W.P. Schleich, Quantum Optics in Phase Space, Wiley-VCH, Berlin, 2001.
- [3] M.O. Scully, M.S. Zubairy, Quantum Optics, Cambridge University Press, Cambridge, England, 1997.
- [4] A. Walther, J. Opt. Soc. Am. 58 (1968) 1256.
- [5] A.T. Friberg, J. Opt. Soc. Am. 69 (1979) 192.
- [6] L. Mandel, E. Wolf, Optical Coherence and Quantum Optics, Cambridge University Press, Cambridge, UK, 1995.
- [7] D. Dragoman, Prog. Opt. 37 (1997) 1.
- [8] A. Torre, Linear Ray and Wave Optics in Phase Space, Elsevier, Amsterdam, 2005.
- [9] M.J. Bastiaans, Opt. Commun. 25 (1978) 26.
- [10] M.J. Bastiaans, J. Opt. Soc. Am. 69 (1979) 1710.
- [11] R. Simon, N. Mukunda, J. Opt. Soc. Am. A 17 (2000) 2440.
- [12] A. Luis, Eur. J. Phys. 28 (2007) 231.
- [13] A. Luis, Phys. Rev. A 76 (2007) 043827.
- [14] A. Luis, Opt. Commun. 266 (2006) 426.
- [15] E.C.G. Sudarshan, Physica A 96 (1979) 315.
- [16] E.C.G. Sudarshan, Phys. Rev. A 23 (1981) 2802.
- [17] E.C.G. Sudarshan, Phys. Lett. A 73 (1979) 269.
- [18] A. Luis, J. Opt. Soc. Am. A 23 (2006) 2855.
- [19] A. Luis, J. Opt. Soc. Am. A 24 (2007) 2070.
- [20] A. Luis, Opt. Lett. 33 (2008) 1497.
- [21] F.J. Torcal-Milla, L.M. Sanchez-Brea, E. Bernabeu, Appl. Opt. 46 (2007) 3668.
- [22] L.M. Sanchez-Brea, F.J. Torcal-Milla, E. Bernabeu, Opt. Commun. 278 (2007) 23.

- [23] L.M. Sanchez-Brea, F.J. Torcal-Milla, E. Bernabeu, J. Opt. Soc. Am. A 25 (2008) 828.
- [24] F.J. Torcal-Milla, L.M. Sanchez-Brea, E. Bernabeu, J. Opt. Soc. Am. A 25 (2008) 2390.
- [25] N. Mukunda, Am. J. Phys. 47 (1979) 182.
- [26] J.P. Bizarro, Phys. Rev. A 49 (1994) 3255.
- [27] P. Kasperkovitz, M. Peev, Ann. Phys. NY 230 (1994) 21.
- [28] A. Lukš, V. Peřinová, Quant. Opt. 6 (1994) 125.
- [29] U. Leonhardt, Phys. Rev. Lett. 74 (1995) 4101.
- [30] U. Leonhardt, Phys. Rev. A 53 (1996) 2998.
- [31] J. Ojeda-Castañeda, E.E. Sicre, Opt. Acta 32 (1985) 17.
- [32] M. Testorf, J. Ojeda-Castañeda, J. Opt. Soc. Am. A 13 (1996) 119.
- [33] K. Banaszek, K. Wódkiewicz, W.P. Schleich, Opt. Express 2 (1998) 169.
- [34] V. Arrizón, G. Rojo-Velázquez, J. Opt. Soc. Am. A 18 (2001) 1252.
- [35] P. Beckmann, A. Spizzichino, The Scattering of Electromagnetic Waves from Rough Surfaces, Artech House, Norwood, 1987.